A Critical Discussion of the Continuous-Discrete Extended Kalman Filter

John Bagterp Jørgensen
Informatics and Mathematical Modelling
Technical University of Denmark
DK-2800 Kgs. Lyngby, Denmark
jbj@imm.dtu.dk

***Abstract*— In this paper, we derive and apply a novel numerically robust and computationally efficient extended Kalman filter for state estimation in nonlinear continuous-discrete stochastic systems. The continuous-discrete extended Kalman filter is applied to the Van der Vusse reaction example. This example is a well-known benchmark for nonlinear predictive control. Using the Van der Vusse example, we demonstrate inherent limitations of the extended Kalman filter and sensor structure for unbiased state estimation. In particular, we demonstrate that the convergence rate of the concentration estimate in the Van der Vusse system is limited by the frequency of concentration measurements. These limitations limit the achievable performance of any closed-loop system including nonlinear model predictive control.**

I. Introduction

The objective of state estimation is to reconstruct the state of a system from process measurements given a model. State estimation has important applications in nonlinear model predictive control as well as in monitoring, prediction and fault detection of chemical processes. Several approaches to state estimation in systems modelled by ordinary differential equations exist. They include a rigorous probabilistic method solving Kolmogorov's (Fokker-Planck's) forward equation [1], [2] as well as approximative methods such as extended Kalman filtering (EKF) [3], [4] and optimization based approaches usually referred to as moving horizon estimation (MHE) [5]–[8]. The probabilistic approach based on solution of Kolmogorov's forward equation is applicable only to the simplest systems due to its requirement for solution of partial differential equations with the number of independent variables equal to the number of stochastic states. Moving horizon estimation has gained some popularity recently due to its similarity to model predictive control and its ability to handle constraints on the states and the stochastic process disturbances. Undoubtedly, the extended Kalman filter is the most widely adopted state estimation technology for nonlinear systems and remains the standard technology for state estimation in nonlinear model predictive control applications despite recent popularity of moving horizon estimation [9]–[12]. Furthermore, systematic methods for grey-box identification of nonlinear models used in continuous-discrete time extended Kalman filters exist [13]–[15].

The state estimate quality of any of these state estimation techniques is limited by plant-model mismatch including unmeasured disturbances as well as the underlying sensor structure providing the feedback. These limitations and the expected performance of a continuous-discrete EKF are illustrated for the Van der Vusse benchmark example.

This paper is organized as follows. Section II introduces the extended Kalman filter for continuous-discrete stochastic systems. In Section III, we demonstrate the performance of the continuous-discrete EKF and provide a critical discussions of its limitations in process control applications. Section IV provides the conclusions.

II. Continuous-Discrete EKF

Consider the continuous-discrete stochastic nonlinear system

$$d\boldsymbol{x}(t) = f(t, \boldsymbol{x}(t))dt + \sigma(t)d\boldsymbol{\omega}(t) \tag{1a}$$

$$\boldsymbol{y}_k = h(t_k, \boldsymbol{x}(t_k)) + \boldsymbol{v}_k \tag{1b}$$

in which $\{\boldsymbol{\omega}(t),\, t \geq 0\}$ is a standard Wiener process, i.e. a Wiener process with incremental covariance Idt, and the measurement noise is normally distributed, $\boldsymbol{v}_k = \boldsymbol{v}(t_k) \sim N_{iid}(0, R_k)$. Assume that the mean and covariance of the initial state are known, i.e.

$$\boldsymbol{x}_{0|-1} \sim \mathbb{F}(\hat{x}_{0|-1}, P_{0|-1}) \tag{1c}$$

Then the extended Kalman filter for filtering and prediction in (1) may be stated as follows. The one-step ahead prediction of the measurement, $\hat{y}_{k|k-1} = y_{k-1}(t_k)$, and its approximate covariance, $R_{k|k-1}$, are computed as

$$\hat{y}_{k|k-1} = h(t_k, \hat{x}_{k|k-1}) \tag{2a}$$

$$C_k = \frac{\partial h}{\partial x}(t_k, \hat{x}_{k|k-1}) \tag{2b}$$

$$R_{k|k-1} = C_k P_{k|k-1} C_k' + R_k \tag{2c}$$

The innovation, e_k, is obtained by

$$e_k = y_k - \hat{y}_{k|k-1} \tag{3}$$

and the state filter gain is computed using the expression

$$K_{fx,k} = P_{k|k-1} C_k' R_{k|k-1}^{-1} \tag{4}$$

The filtered state, $\hat{x}_{k|k}$, and its covariance, $P_{k|k}$, are computed by

$$\hat{x}_{k|k} = \hat{x}_{k|k-1} + K_{fx,k} e_k \tag{5a}$$

$$P_{k|k} = P_{k|k-1} - K_{fx,k} R_{e,k} K_{fx,k}' \tag{5b}$$

The above formulas for the measurement update is structurally equivalent to the discrete-time case. The difference between the discrete-time case and the continuous-discrete time case arises in the one-step ahead propagation of the state estimate and its covariance. In the continuous-discrete case $\hat{x}_{k+1|k} = \hat{x}_k(t_{k+1}) = \hat{x}(t_{k+1}; t_k, \hat{x}_{k|k})$ and $P_{k+1|k} = P_k(t_{k+1}) = P(t_{k+1}; t_k, \hat{x}_{k|k}, P_{k|k})$ are computed as the solution to the system of differential equations

$$\frac{d\hat{x}_k(t)}{dt} = f(t, \hat{x}_k(t)) \tag{6a}$$

$$\frac{dP_k(t)}{dt} = A(t)P_k(t) + P_k(t)A(t)' + \sigma(t)\sigma(t)' \tag{6b}$$

in which

$$A(t) = \frac{\partial f}{\partial x}(t, \hat{x}_k(t)) \tag{6c}$$

and with initial conditions $\hat{x}_k(t_k) = \hat{x}_{k|k}$ and $P_k(t_k) = P_{k|k}$. The main computational effort in the extended Kalman filter is the solution of (6). While this system can be solved using software for the standard initial value problem for systems of ordinary differential equations, it is highly inefficient to do so as (6) has additional structure that may be utilized for its efficient solution. We apply a specialized explicit singly diagonal implicit Runge-Kutta solver, ESDIRK, for solution of this system [16], [17].

A. Array Algorithm

Computational efficiency in terms of speed is only one concern for the numerical solution of (6) embodied in an extended Kalman algorithm for state estimation in the system (1). As the algorithm is to be executed unsupervised in a real-time control system, numerical stability and robustness are just as important as computational speed. Therefore, the numerical robust array algorithm which propagates the matrix square roots of the covariances rather than the covariances themselves is preferred [4].

The steps in the array algorithm are as follows. The one-step ahead prediction of the measurement vector and its derivative are

$$\hat{y}_{k|k-1} = h(t_k, \hat{x}_{k|k-1}) \tag{7a}$$

$$C_k = \frac{\partial h}{\partial x}(t_k, \hat{x}_{k|k-1}) \tag{7b}$$

Using an orthogonal transformation, $R^{1/2}_{k|k-1}$, $\bar{K}_{fx,k}$ and $P^{1/2}_{k|k}$ are computed as

$$\begin{bmatrix} R_k^{1/2} & C_k P^{1/2}_{k|k-1} \\ 0 & P^{1/2}_{k|k-1} \end{bmatrix} \Theta_M = \begin{bmatrix} R^{1/2}_{k|k-1} & 0 \\ \bar{K}_{fx,k} & P^{1/2}_{k|k} \end{bmatrix} \tag{8}$$

and the filtered state, $\hat{x}_{k|k}$, is computed by

$$e_k = y_k - \hat{y}_{k|k-1} \tag{9a}$$

$$\bar{e}_k = \left(R^{1/2}_{k|k-1}\right)^{-1} e_k \tag{9b}$$

$$\hat{x}_{k|k} = \hat{x}_{k|k-1} + \bar{K}_{fx,k}\bar{e}_k \tag{9c}$$

Algorithm 1 Square root algorithm for $P_{k+1|k}$ in (11).

$\begin{bmatrix} X^{1/2} & 0 \end{bmatrix} \leftarrow \begin{bmatrix} \Phi(t_{k+1}, t_k)P^{1/2}_{k|k} & \Phi(t_{k+1}, T_1)\sqrt{\delta_1}Q_1^{1/2} \end{bmatrix} \Theta_1$
for $i = 2 : n_q$ **do**
  $\begin{bmatrix} X^{1/2} & 0 \end{bmatrix} \leftarrow \begin{bmatrix} X^{1/2} & \Phi(t_{k+1}, T_i)\sqrt{\delta_i}Q_i^{1/2} \end{bmatrix} \Theta_i$
end for
$P^{1/2}_{k+1|k} \leftarrow X^{1/2}$

Instead of computing the one-step ahead prediction of the states and the associated covariance by (6), ESDIRK computes these quantities by the following equivalent set of equations

$$\frac{d\hat{x}_k(t)}{dt} = f(t, \hat{x}_k(t)) \quad \hat{x}_k(t_k) = \hat{x}_{k|k} \tag{10a}$$

$$\frac{d\Phi(t,s)}{dt} = A(t)\Phi(t,s) \quad \Phi(s,s) = I \tag{10b}$$

in which

$$A(t) = \frac{\partial f}{\partial x}(t, \hat{x}_k(t)) \tag{10c}$$

and

$$\begin{aligned} P_k(t) = {} & \Phi(t, t_k)P_{k|k}\Phi(t, t_k)' \\ & + \int_{t_k}^{t} \Phi(t,s)\sigma(s)\sigma(s)'\Phi(t,s)'ds \end{aligned} \tag{10d}$$

The equivalence of (6) and (10) follows directly from the derivation of (6) [17], [18]. Equation (10b) has almost the same structure as the state sensitivity equation. However, in (10b) the initial time is also variable. If the integral of (10d) is computed by quadrature then it may be expressed as

$$\begin{aligned} P_{k+1|k} &= P_k(t_{k+1}) \\ &= \Phi(t_{k+1}, t_k)P_{k|k}\Phi(t_{k+1}, t_k)' \\ &\quad + \int_{t_k}^{t_{k+1}} \Phi(t_{k+1}, s)Q(s)\Phi(t_{k+1}, s)'ds \\ &\approx \Phi(t_{k+1}, t_k)P_{k|k}\Phi(t_{k+1}, t_k)' \\ &\quad + \sum_{i=1}^{n_q} \delta_i \Phi(t_{k+1}, T_i)Q(T_i)\Phi(t_{k+1}, T_i)' \end{aligned} \tag{11}$$

in which $Q(s) = \sigma(s)\sigma(s)'$ and n_q is the number of quadrature points. Let $Q_i = Q(T_i)$. Then it is evident from (11) that the one-step ahead covariance square root, $P^{1/2}_{k+1|k}$, can be computed by a sequence of orthogonal transformations as described in Algorithm 1. In this algorithm, Θ_i are orthogonal transformation operators.

III. Example: Van der Vusse Reaction

In this section, we test the developed extended Kalman filter algorithm on the Van der Vusse reaction. The purpose is to provide a critical evaluation on the application of the ESDIRK based extended Kalman filter. We demonstrate the limitations that the sensor configuration imposes on the state estimation quality and its rate of convergence toward the true value. These limitations also limits the resulting closed-loop performance achievable by any controller including a

TABLE I
PARAMETERS FOR THE VAN DER VUSSE CSTR.

Symbol	Value	Symbol	Value
k_{10}	$1.287 \cdot 10^{12}$ hr^{-1}	ρ	0.9342 kg/L
k_{20}	$1.287 \cdot 10^{12}$ hr^{-1}	C_p	3.01 $\frac{\text{kJ}}{\text{kg}\cdot\text{K}}$
k_{30}	$9.043 \cdot 10^{9}$ $\frac{\text{L}}{\text{hr}\cdot\text{mol}}$	k_w	4032 $\frac{\text{kJ}}{\text{hr}\cdot\text{m}^2\cdot\text{K}}$
E_1/R	9758.3 K	A_R	0.215 m^2
E_2/R	9758.3 K	V_R	10 L
E_3/R	8560 K	m_J	5 kg
ΔH_{r_1}	4.2 kJ/mol	C_{PJ}	2.0 $\frac{\text{kJ}}{\text{kg}\cdot\text{K}}$
ΔH_{r_2}	-11.0 kJ/mol	c_{A0}	5.1 mol/L
ΔH_{r_3}	-41.85 kJ/mol	T_0	378.05 K

TABLE II
NOMINAL STEADY STATE FOR THE VAN DER VUSSE CSTR.

Symbol	Value	Symbol	Value
c_A	2.1404 mol/L	F	141.9 L/hr
c_B	1.0903 mol/L	$\dot{Q}_J$	-1113.5 kJ/hr
T	387.34 K	c_{A0}	5.1 mol/L
T_J	386.06 K	T_0	378.05 K

nonlinear predictive controller. The Van der Vusse reaction has been exploited in several controller benchmark studies [19]–[22]. The Van der Vusse reaction is

$$A \xrightarrow{k_1} B \xrightarrow{k_2} C$$
$$2A \xrightarrow{k_3} D$$

in which B is the desired product, while C and D are unwanted by-products. The reaction is conducted in a CSTR with a cooling jacket. The reaction rates for this system are

$$r_1(T, c_A) = k_1(T)c_A, k_1(T) = k_{10} \exp\left(-\frac{E_1}{RT}\right) \quad (12a)$$

$$r_2(T, c_B) = k_2(T)c_B, k_2(T) = k_{20} \exp\left(-\frac{E_2}{RT}\right) \quad (12b)$$

$$r_3(T, c_A) = k_3(T)c_A^2, k_3(T) = k_{30} \exp\left(-\frac{E_3}{RT}\right) \quad (12c)$$

and the model of the CSTR is

$$\dot{c}_A = \frac{F}{V_R}(c_{A0} - c_A) - r_1(T, c_A) - r_3(T, c_A) \quad (13a)$$

$$\dot{c}_B = -\frac{F}{V_R} c_B + r_1(T, c_A) - r_2(T, c_B) \quad (13b)$$

$$\dot{T} = \frac{F}{V_R}(T_0 - T) + \frac{k_w A_R}{\rho C_p V_R}(T_J - T) - \frac{r_1(T, c_A)\Delta H_{r_1} + r_2(T, c_B)\Delta H_{r_2} + r_3(T, c_A)\Delta H_{r_3}}{\rho C_p} \quad (13c)$$

$$\dot{T}_J = \frac{1}{m_J C_{PJ}} \left(\dot{Q}_J + k_w A_R (T - T_J)\right) \quad (13d)$$

The parameters and nominal operating point are provided in Tables I and II, respectively.

The model of the Van der Vusse system is a deterministic system of ordinary differential equations, i.e.

$$\frac{dx(t)}{dt} = f(x(t), u(t), d(t)) \quad (14)$$

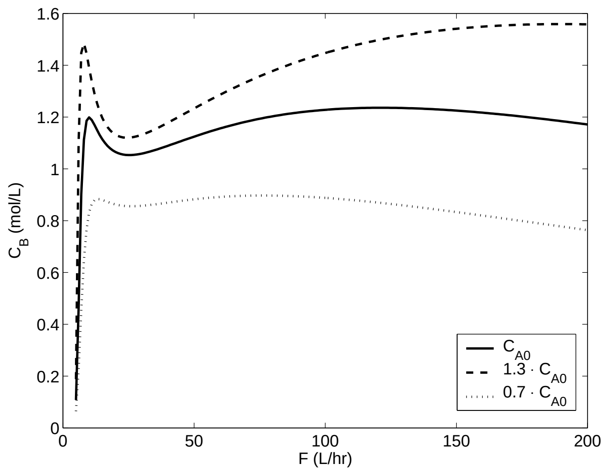

Fig. 1. Steady state plot for the concentration of B.

in which

$$x = \begin{bmatrix} c_A \\ c_B \\ T \\ T_J \end{bmatrix} \quad u = \begin{bmatrix} F \\ \dot{Q}_J \end{bmatrix} \quad d = \begin{bmatrix} c_{A0} \\ T_0 \end{bmatrix}$$

and x is the state vector, u is the manipulable input vector, and d is the disturbance vector. The steady state yield of B as function of the feed flow rate for different values of the feed concentration of A is plotted in Figure 1. It should be noted that around the optimal point of operation (maximum yield), the gain from the feed flow rate to the concentration of B changes sign. Hence, the system is not integral controllable by a linear controller in that optimal operating point.

The deterministic system (14) is augmented by a stochastic term, $\sigma d\boldsymbol{\omega}(t)$, describing the random part of the state evolution. Consequently, the evolution of the Van der Vusse system is described by the following system of stochastic differential equations

$$d\boldsymbol{x}(t) = f(\boldsymbol{x}(t), u(t), d(t))dt + \sigma d\boldsymbol{\omega}(t) \quad (15)$$

A stochastic and deterministic simulation of the Van der Vusse system is plotted in Figure 2. At time $t = 4.0$, the feed concentration of A is increased by 20%. The diffusion term is selected as $\sigma = 0.03\text{diag}(x_0)$[1] and the stochastic system is simulated using the Euler-Maruyama scheme with a step length of 0.0001 hr [23].

The stochastic differential equation (15) is observed by the following stochastic measurement equation

$$\boldsymbol{y}(t_k) = h(\boldsymbol{x}(t_k)) + \boldsymbol{v}(t_k) \quad \boldsymbol{v}(t_k) \sim N(0, R_k) \quad (16)$$

at the discrete times $\{t_k = 0.01k : k = 0, 1, \ldots\}$. The measurement noise covariance, R_k, is a diagonal matrix with the entries equal to 0.1 times the corresponding entries in σ, i.e. for the full state measurement case $R_k = 0.1\sigma$. The measurement scenario used for the simulations is illustrated in Figure 3. In the full state feedback all measurements

[1]Using the Matlab notion of diag.

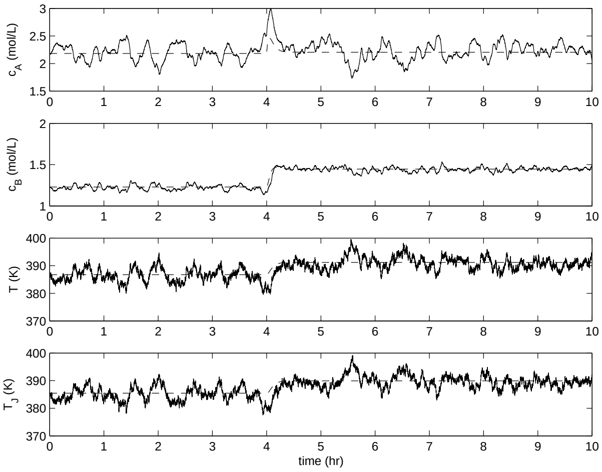

Fig. 2. Stochastic and deterministic (dashed line) simulation of the Van der Vusse system.

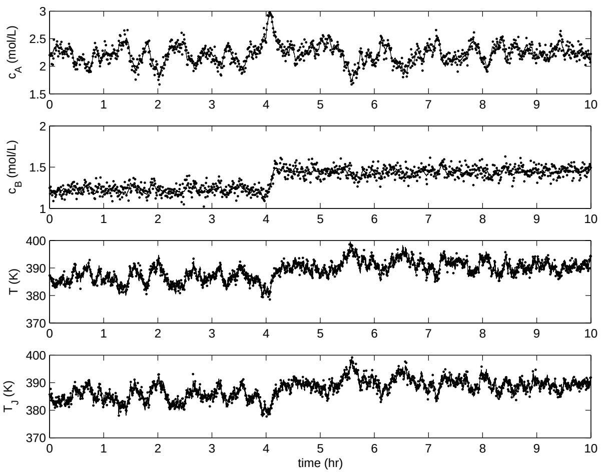

Fig. 3. Noise corrupted measurements (dots) and actual states (full line) for the Van der Vusse system.

are used for the extended Kalman filter, while only the temperature measurements are used for the extended Kalman filter in the temperature feedback case.

Systematic procedures for identification of parameters in continuous-discrete stochastic systems (15)-(16) exist but is outside the topic of this paper [14], [15].

A. Temperature and Concentration Feedback

The first case considered is the case with full state feedback, i.e. all states are measured; though the measurements are corrupted by measurement noise. The filtered estimate of the states, $\hat{x}_{k|k}$, and true states are illustrated in Figure 4. The filtered state estimate is close to the true state until time $t = 4.0$ at which the disturbance in the feed concentration of A occurs. After that time, at which there is a plant-model mismatch, a significant offset in the estimation of the concentrations of A and B persists.

To avoid the persistent offset of the concentration estimates in the case of unknown disturbances, i.e. plant-model

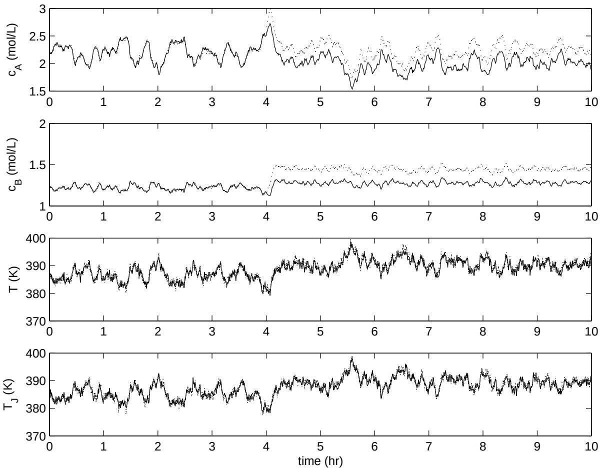

Fig. 4. The filter estimates and the true states (dotted line) for the case with full state feedback and no integrators.

mismatch, the model is augmented with integrators [24], [25]. In this case, we augment the model with integrators in the feed concentration of A, c_{A0}, and the feed temperature, T_0, i.e. integrators in the unmeasured disturbance vector, d. Hence, in the framework of stochastic differential equations, the integrator states, $\boldsymbol{x}_d(t)$, used for estimating d is a random walk

$$d\boldsymbol{x}_d(t) = \sigma_d d\boldsymbol{\omega}_d(t) \qquad (17)$$

such that the augmented model becomes

$$d\begin{bmatrix}\boldsymbol{x}(t)\\ \boldsymbol{x}_d(t)\end{bmatrix} = \begin{bmatrix} f(\boldsymbol{x}(t), u(t), \boldsymbol{x}_d(t)) \\ 0 \end{bmatrix} dt + \begin{bmatrix}\sigma & 0 \\ 0 & \sigma_d\end{bmatrix} d\begin{bmatrix}\boldsymbol{\omega}(t)\\ \boldsymbol{\omega}_d(t)\end{bmatrix} \qquad (18)$$

This model augmented with integrators is used by the extended Kalman filter for state estimation with $\sigma_d = 0.01d$, $(\hat{x}_d)_{0|-1} = d$, and the corresponding covariance matrix equal to the unity matrix. The filtered state estimates and the true states are illustrated in Figure 5. The estimated disturbances and their true values are plotted in Figure 6. In this case, there is no persistent offset in the state estimates and the estimates of the unknown disturbances converge to their true values. In conclusion, the extended kalman filter performs adequately as a state estimator for this system with full noise corrupted state feedback and unknown disturbances in the feed concentration of A.

B. Temperature Feedback

Consider the more realistic situation in which the concentrations of A and B are not measured. Only the temperatures T and T_J are measured. The performance of the continuous-discrete extended Kalman filter with input integrators deteriorate dramatically. This is illustrated in Figures 7 and 8. The filtered state estimates for the concentrations as well as the unknown input disturbances do not converge to their true values. Provided that the system is locally detectable with the available measurements and that the noise model is locally stabilizable the estimated states converge in a mean sense. However, even though it is in principle possible to

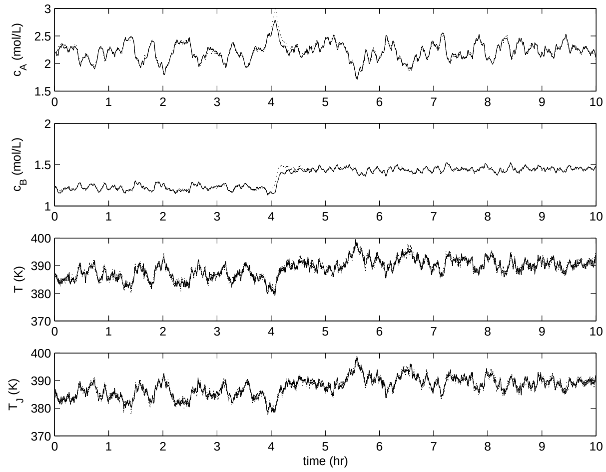

Fig. 5. The filter estimates and the true states (dotted line) for the case with full state feedback and two input disturbance integrators.

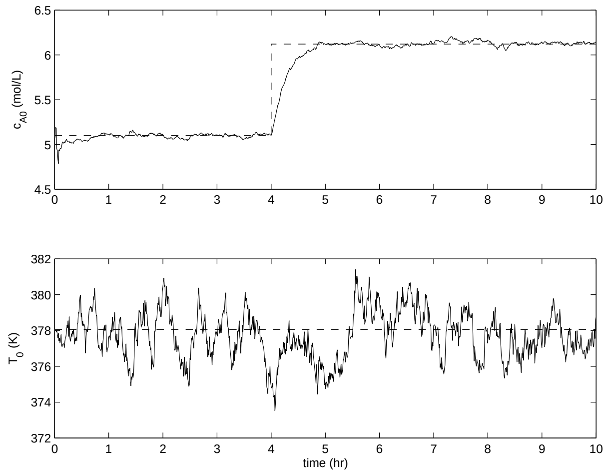

Fig. 6. The filter estimates of the two input integrators and their true value (dashed line) for the case with full state feedback.

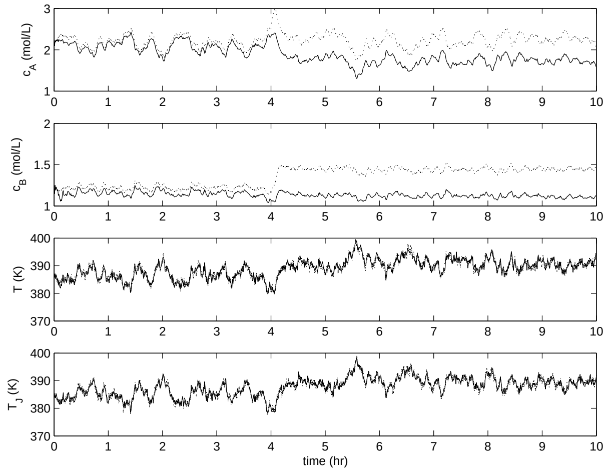

Fig. 7. The filter estimates and the true states (dotted line) for the case with only temperature feedback and two input disturbance integrators.

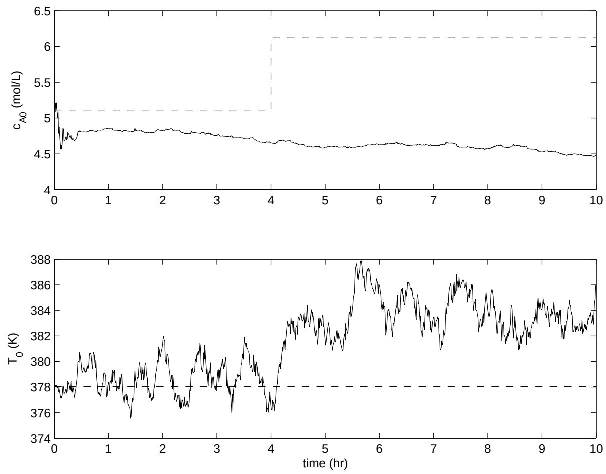

Fig. 8. The filter estimates of the two input integrators and their true value (dashed line) for the case with only temperature feedback.

estimate the unmeasured states from the subset of measured states, it is often so in practice that in the face of model-plant mismatch the result is quite disappointing in the sense that one cannot substitute concentration measurements with a soft sensor such as the EKF [26]. There is simply no substitute for a good sensor (except for the Utopian wish for a perfect model).

C. Laboratory Measurement of the Concentrations

To overcome some of the limitations associated with an estimator based on only temperature measurements, we assume that the concentrations are measured every 15 minutes (25 times less frequent than the sample rate of the EKF). This setup is supposed to emulate the situation in which the concentrations, c_A and c_B, are measured by a laboratory procedure[2]. The resulting performance of the extended Kalman filter with input disturbance integrators is illustrated in figures 9 and 10. While the filtered state and input disturbance estimates converge to their true values, the convergence is slower compared to the full state feedback case. This observation is not surprising, but points to the fact that the achievable performance of a closed-loop feedback system intended to control either the productivity or the concentration of B is ultimately limited by the rate at which the estimates of c_B, c_A, and c_{A0} converge. And the convergence rate is limited by the frequency at which the concentrations are measured.

IV. Conclusion

A numerically robust and efficient extended Kalman filter has been introduced as an approximative technique for state estimation in nonlinear stochastic continuous-discrete systems (1). The continuous-discrete extended Kalman filter is applied to the Van der Vusse benchmark example. In this example, temperature measurements are *not* sufficient

[2] A more realistic emulation would include time delay due to the laboratory procedure. To keep the setup simple, the analysis time is assumed negligible in this study.

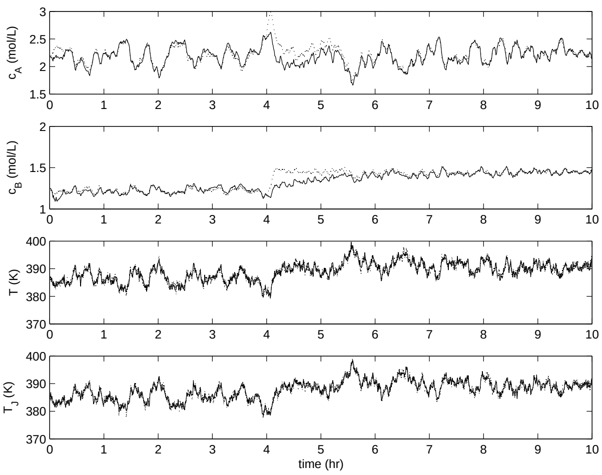

Fig. 9. The filter estimates and the true states (dotted line) for the case with frequent temperature measurements, infrequent concentration measurements, and two input disturbance integrators.

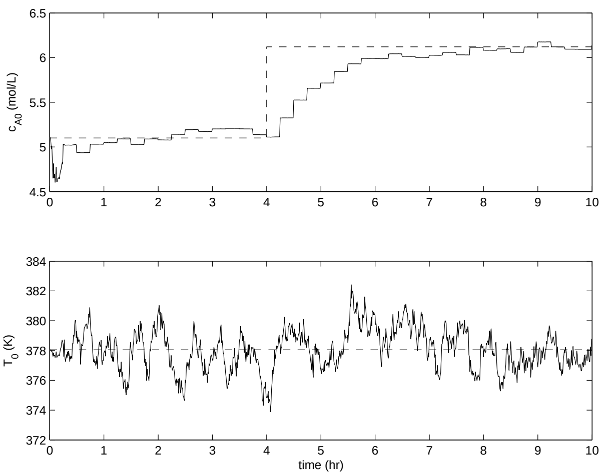

Fig. 10. The filter estimates of the two input integrators and their true value (dashed line) for the case with frequent temperature measurements and infrequent concentration measurements.

to provide steady-state offset free state estimation. The convergence rate of the concentration estimates is limited by the frequency of concentration measurements. This implies that the closed-loop performance of the Van der Vusse benchmark for any controller including nonlinear predictive control is limited by the concentration measurement frequency.

REFERENCES

[1] A. H. Jazwinski, *Stochastic Processes and Filtering Theory*. Academic Press, 1970.

[2] P. S. Maybeck, *Stochastic Models, Estimation, and Control*. London: Academic Press, 1982.

[3] W. H. Sorenson, Ed., *Kalman Filtering: Theory and Application*. London: IEEE Press, 1985.

[4] T. Kailath, A. H. Sayed, and B. Hassibi, *Linear Estimation*. Prentice Hall, 2000.

[5] S.-S. Jang, B. Joseph, and H. Mukai, "Comparison of two approaches to on-line parameter and state estimation of nonlinear systems," *Ind. Eng. Chem. Process Des. Dev.*, vol. 25, pp. 809–814, 1986.

[6] C. V. Rao and J. B. Rawlings, "Nonlinear moving horizon state estimation," in *Nonlinear Model Predictive Control*, F. Allgöwer and A. Zheng, Eds. Basel: Birkhäuser, 2000, pp. 45–69.

[7] C. V. Rao, J. B. Rawlings, and J. H. Lee, "Constrained linear state estimation - a moving horizon approach," *Automatica*, vol. 37, pp. 1619–1628, 2001.

[8] E. L. Haseltine and J. B. Rawlings, "Critical evaluation of extended kalman filtering and moving-horizon estimation," *Ind. Eng. Chem. Res.*, vol. 44, pp. 2451–2460, 2005.

[9] D. Dochain, "State and parameter estimation in chemical and biochemical processes: A tutorial," *Journal of Process Control*, vol. 13, pp. 801–818, 2003.

[10] J. H. Lee and N. L. Ricker, "Extended kalman filter based nonlinear model predictive control," *Ind. Eng. Chem. Res.*, vol. 33, p. 1530, 1994.

[11] J. Valappil and C. Georgakis, "Systematic estimation of state noise statistics for extended kalman filters," *AIChE Journal*, vol. 46, p. 292, 2000.

[12] Z. K. Nagy and R. D. Braatz, "Robust nonlinear model predictive control of batch processes," *AIChE Journal*, vol. 49, pp. 1776–1786, 2003.

[13] L. Ljung, *System Identification. Theory for the User*, 2nd ed. Upper Saddle River, NJ: Prentice Hall, 1999.

[14] N. R. Kristensen, H. Madsen, and S. B. Jørgensen, "Parameter estimation in stochastic grey-box models," *Automatica*, vol. 40, pp. 225–237, 2004.

[15] ——, "A method for systematic improvement of stochastic grey-box models," *Computers and Chemical Engineering*, vol. 28, pp. 1431–1449, 2004.

[16] M. R. Kristensen, J. B. Jørgensen, P. G. Thomsen, and S. B. Jørgensen, "An ESDIRK method with sensitivity analysis capabilities," *Computers and Chemical Engineering*, vol. 28, pp. 2695–2707, 2004.

[17] J. B. Jørgensen, M. R. Kristensen, P. G. Thomsen, and H. Madsen, "A computationally efficient and robust implementation of the continuous-discrete extended kalman filter," in *Submitted for ACC 2007*, 2007.

[18] K. J. Åström, *Introduction to Stochastic Control Theory*. New York: Academic Press, 1970.

[19] K.-U. Klatt and S. Engell, "Rührkesselreaktor mit parallel- und folgereaktionen," in *Nichtlineare Regelung - Methoden, Werkzeuge, Anwendungen*, ser. VDI-Berichte Nr. 126, S. Engell, Ed. Düsseldorf: VDI-Verlag, 1993, pp. 101–108.

[20] S. Engell and K.-U. Klatt, "Nonlinear control of a nonminimum phase CSTR," in *Proceedings of the American Control Conference*, 1993, p. 2941.

[21] B. A. Ogunnaike and W. H. Ray, *Process Dynamics, Modeling, and Control*. New York: Oxford University Press, 1994.

[22] H. Chen, A. Kremling, and F. Allgöwer, "Nonlinear predictive control of a benchmark CSTR," in *Proceedings of the 3rd European Control Conference ECC'95*, 1995, pp. 3247–3252.

[23] P. E. Kloeden and E. Platen, *Numerical Solution of Stochastic Differential Equations*. Berlin: Springer, 1995.

[24] G. Pannocchia and J. B. Rawlings, "Disturbance models for offset-free model-predictive control," *AIChE J.*, vol. 49, pp. 426–437, 2003.

[25] K. R. Muske and T. A. Badgwell, "Disturbance modeling for offset-free linear model predictive control," *Journal of Process Control*, vol. 12, pp. 617–632, 2002.

[26] D. I. Wilson, M. Agarwal, and D. W. T. Rippin, "Experiences implementing the extended kalman filter on an industrial batch reactor," *Computers and Chemical Engineering*, vol. 22, pp. 1653–1672, 1998.